University of Kentucky Master's Theses   Graduate School

2007

ROLE OF CONDUCTION IN THE GENESIS OF ALTERNANS OF ACTION POTENTIAL DURATION IN A SIMULATED ONE DIMENSIONAL FIBER

Sanjiv Ramalingam
University of Kentucky, sanjiv_2k@yahoo.com

ABSTRACT OF THESIS

ROLE OF CONDUCTION IN THE GENESIS OF ALTERNANS OF ACTION POTENTIAL DURATION IN A SIMULATED ONE DIMENSIONAL FIBER

Ventricular fibrillation is one of the leading causes for Sudden Cardiac Death and is characterized by multiple activation wavefronts. Multiple activation wavefronts originate from a reentrant circuit which requires the presence of a unidirectional block in the path of a propagating excitation wave. It has been proposed that at the cellular level beat to beat alternation in the action potential duration at rapid pacing rates can result in a conduction block. Various mechanisms have been postulated to show the mechanisms of alternans. We use simulated activation in a one dimensional tissue fiber to show the existence of a new mechanism via which alternans can result. We used a new pacing protocol to eliminate alternans at the pacing site, and thus eliminating restitution of action potential duration at this site to reveal existence of alternans down the fiber. Effects on alternans of manipulations of specific ionic currents such as the sodium current (I_{Na}), calcium current (I_{CaL}), potassium current (I_{kr}) and of the diffusion co-efficient (D_x) which simulates reduced expression of connexin 43 were determined. Decrease in sodium conductance, i.e. in excitability by half caused the alternans to occur at the pacing site itself even though APD restitution was eliminated. An increase or decrease in calcium current (I_{CaL}) eliminated alternans throughout the fiber. The use of a novel pacing approach in investigation of alternans, as in this study, furthers our understanding of the mechanism of alternans and may prove helpful in the development of better anti-arrhythmic drugs in the future.

KEYWORDS: Ventricular fibrillation, reentrant circuit, unidirectional block, alternans, anti-arrhythmic

Sanjiv Ramalingam

04/18/2007

ROLE OF CONDUCTION IN THE GENESIS OF ALTERNANS OF ACTION
POTENTIAL DURATION IN A SIMULATED ONE DIMENSIONAL FIBER

By

Sanjiv Ramalingam

<u>Dr. Abhijit Patwardhan</u>

Director of Thesis

Director of Graduate
Studies

<u>04/18/2007</u>

RULES FOR THE USE OF THESES

THESIS

Sanjiv Ramalingam

The Graduate School

University of Kentucky

2007

ROLE OF CONDUCTION IN THE GENESIS OF ALTERNANS OF ACTION
POTENTIAL DURATION IN A SIMULATED ONE DIMENSIONAL FIBER

_____

THESIS

_____

A thesis submitted in partial fulfillment of the requirements for the degree of
Master of
Science in the Graduate School at the University of Kentucky

Graduate School

at the University of Kentucky

By

Sanjiv Ramalingam

Advisor: Dr. Abhijit Patwardhan

Lexington, Kentucky

April 2007

ACKNOWLEDGEMENTS

I would like to thank and extend my gratitude to my advisor and professor, Dr. Abhijit Patwardhan. His guidance, support and perseverance through the course of my research were invaluable. I am thankful to him for having offered me such an incredible opportunity. Without his assistance I would not have earned this valuable degree.

I would also like to thank the members of my committee Dr. Charles Knapp and Dr. Jonathan Satin for their valuable suggestions and support.

And finally to my mother and father without whose love and support I would not have been here.

TABLE OF CONTENTS

LIST OF FIGURES

LIST OF FILES

Chapter One: Introduction

Beat by beat alternation in action potential duration (APD), which is known as alternans of APD have been shown to be closely linked with onset of ventricular arrhythmia and sudden cardiac death [1-5]. It has been proposed that at the cellular level, beat to beat alternation in APD that occurs at rapid pacing rates can result in conduction block [6].

Various mechanisms of alternation of cardiac APD have been reported. One of the well known mechanisms is the restitution hypothesis [7]. The restitution hypothesis states that a necessary condition for instability or alternans to occur is that the slope of the restitution curve should be greater than or equal to 1. An implication of this hypothesis is that if the slope of the restitution curve is less than 1 the heart rhythm would be anti-arrhythmic. Some studies have shown anti-arrhythmic effects of drugs that decrease slope of restitution, consistent with the hypothesis [8, 9]. However, recent experimental studies in canines, in which alternans of APD was observed even when the diastolic interval (DI) preceding the action potentials were constant, questions the validity of APD restitution as a "necessary" mechanism of alternans of APD. The above study revealed the existence of a restitution independent component of alternans [10]. In addition to the restitution hypothesis, the interplay between restitution of conduction velocity (CV) and restitution of APD is also thought to influence alternans importantly [11]. Conduction velocity is the time taken for a depolarization charge to travel a unit distance. Typically the unit is mm/msec. Conduction velocity across the myocardium is not uniform and varies across species and also with respect to the fiber orientation [12]. Restitution of CV is the dependence of CV on DI. Typically the CV decreases with lower DIs. The CV restitution curve is obtained using the standard or the dynamic protocols and is similar in procedure to APD restitution with the difference being in the Y co-ordinate. Of the two trajectories namely the APD restitution (figure 3A) and the CV restitution (figure 3B) the CV restitution curve has a much flatter trajectory (slope).

We conducted simulation studies that revealed alternans distal to pacing site in a one dimensional tissue even after eliminating alternans at the pacing site using a novel feedback pacing protocol [13]. We investigated the mechanisms of alternans in this specific situation by varying certain ionic currents that are expected to influence conduction and APD importantly. For each ionic modification, plots of restitution of APD and of conduction velocity were obtained using the standard protocol. These plots were obtained to study the effect of modifications of specific ionic currents on the restitution curves.

Chapter Two: Background

2.1 Sudden Cardiac Death

The primary function of the heart is to pump blood to various parts of the body and it performs this operation by means of an electromechanical process. The mechanical action is always accompanied by means of electrical impulse propagation. Electrical impulses travel from the sino atrial node (the pacemaker) from the right atrium to the left atrium via the Bachmann bundle and with a slight delay to the ventricles via the atrioventricular node, bundle of His and purkinje fibres [14]. Disruption of electrical impulse propagation in this pathway can lead to fatal consequences such as Sudden Cardiac Death.

"Sudden cardiac death (also called sudden arrest) is death resulting from an abrupt loss of heart function (cardiac arrest). About 325,000 people a year die of coronary heart disease (CHD) without being hospitalized or admitted to an emergency room. That's about half of all deaths from CHD — more than 890 Americans each day. Most of these are sudden deaths caused by cardiac arrest. Most of the cardiac arrests that lead to sudden death occur when the electrical impulses in the diseased heart become rapid (ventricular tachycardia) or chaotic (ventricular fibrillation) or both" [15]. These data show that ventricular fibrillation is one of the major causes of sudden cardiac death.

2.2 Ventricular Fibrillation and Restitution

The propagation of electrical charge during ventricular fibrillation is not according to the rhythmic pattern as described above, instead, it is highly unorganized. The ventricles contract in a rapid and unsynchronized manner and is described mechanically more as a "flutter" than as a beat. A person with a fibrillating heart is very highly likely to collapse and experience sudden cardiac death if medical help is not provided within minutes [16]. A high percentage of dangerous arrhythmias have been attributed to the result of a phenomenon known as "re-

entry" [17-21]. Re-entrant activity is characterized by electrical waves that "may rotate uninterruptedly and in a self-sustaining manner to give rise to high frequency electrical activity that propagates throughout the ventricles" [17]. The possible reasons for a re-entrant activity to occur could be the interaction between a propagating electrical wavefront with a block in its path [22, 23] or be initiated by a premature beat [24, 25]. Rapid pacing of the heart is also well known to induce a conduction block [6]. At high pacing rates beat to beat alternation in action potential duration known as alternans is observed. One of the mechanisms that is used to explain alternation of cardiac action potentials is the restitution hypothesis and cardiac electrical restitution is thought to have a major influence on whether an electrical disturbance in the hearts rhythm would degenerate into a re-entrant activity [26].

The restitution curve (figure 3A) is obtained by plotting the action potential duration (APD) of one beat versus the preceding diastolic interval (DI) for that beat (figure 1A). APD restitution is the dependence of APD on DI. Some of the protocols that exist for the obtaining the restitution curve (RC) are the standard protocol [27] and the dynamic protocol [9, 28]. In the standard protocol the cells are paced at a constant cycle length (X) for N beats followed by a single beat of shorter cycle length (Y) and then pacing at X cycle length for another N beats followed a single beat cycle length shorter than Y. This pattern is repeated for shorter and shorter cycle lengths until a point where conduction fails. The RC is obtained by plotting the APD of the 'Y'th beat versus the DI preceding that beat. This is repeated for the succeeding 'Y' beat and so on. In the dynamic protocol instead of a single beat of shorter cycle length after constant cycle length pacing for N beats the single beat of shorter cycle length is replaced also with N beats and the pattern is repeated for shorter and shorter cycle lengths for N beats until block occurs. The RC is obtained by using the APD of the last stimulus for a particular cycle length.

The restitution hypothesis states that a necessary condition for instability or alternans is that the slope of the restitution curve should be greater than or equal to 1 [29, 30].

2.3 Basis of Modeling

Models of cell membrane behavior are often based on the Hodgkin and Huxley model [31] where Kirchhoff's current law (sum of currents entering a node is equal to the sum of the currents leaving the node) is applied. Here the current entering the node would be the stimulus current, I_s which can be expressed as;

$$I_S = I_C + \sum_{X=1}^{X=N} I_X \rightarrow (1)$$

I_C and I_X are the capacitive and X_{th} ionic currents respectively. The capacitive and the ionic currents I_C and I_X can be expanded as follows.

$$I_S = C \frac{dv}{dt} + \sum_{X=1}^{X=N} g_x (v - v_x) \rightarrow (2)$$

C is the capacitance per unit area; V is the membrane voltage; g_x is the conductance of the X_{th} channel which maybe time and voltage dependant and V_X is the equilibrium voltage of the X_{th} channel. The conductances are generally expressed as a function of gating variables, y and can be expressed as,

$$g_y = \hat{g}_y * f_y (y_1, y_2, y_{3,.....}) \rightarrow (3)$$

$\hat{g}_y$'s are experimentally determined constants and f_y's are experimentally determined functions [32].

Chapter Three: Methods and Analysis

We used the Canine Ventricular Model (CVM) developed by Fox et al[33] to simulate electrical activity in a linear strand of 220 cells. Ionic currents were computed individually for each cell using the CVM and the cells were coupled using a diffusion equation[34]. The cell length was set at 200 µm with a diffusion constant of 0.001 cm^2/ms[6]. The one dimensional tissue was stimulated with no flux boundary conditions[35, 36].

The model was paced at 500 ms cycle length for 100 beats to achieve a steady state. Once steady state was reached the protocol was changed from constant cycle length (CL) pacing to a feedback based pacing protocol such that the DI preceding each activation at the pacing site was equal to 40 ms. To achieve feedback control, the location of APD_{90} i.e. the instant when the transmembrane voltage repolarized to 90% of its maximum value was identified. The next stimulus was delivered after a predetermined interval from the point of APD_{90}, this interval became the DI for the next action potential [13, 37]. The tissue was paced such that the DI was constant for each of the 100 beats. Feedback based DI control was established only at the pacing site. The reason for choosing DI equal to 40 msec was because we had previously observed occurrence of alternans experimentally in canines when 40ms of DI preceded activations of alternating duration[10]. A change in APD between successive beats of at least 8 milliseconds was considered as alternans. A standard protocol was used to obtain APD restitution and conduction velocity restitution curves. Briefly, for the standard protocol, the tissue was paced at a constant cycle length (CL) equal to 500 msec (S1) for 50 beats and the interval between the 50th pacing pulse and the 51st pulse was shortened in the following sequence; 500, 400, 300, 250, 220, 210, 200, 190, 185, 180, 175 and 170 ms. For all protocols the pacing stimuli strength was 1.5 times diastolic threshold while for the S1S2 pacing protocol the stimulus strength was 9 times diastolic threshold to ensure that activations occurred at shorter DIs. Custom programs were written in Matlab 7.0 (The

MathWorks, Inc., Natick, MA) for determination of APD_{90} and DI, which were quantified as follows: The time instant when the transmembrane voltage became > -80.5 mv was considered as the start of an action potential. The time instant when the transmembrane voltage repolarized to 90 percent of its maximum value was considered as the end of the action potential. The interval between the end of an action potential and the start of the next action potential became the DI for the next beat (figure 1A). To investigate the role of restitution in genesis of alternans and to compare results with previous studies, first derivative of the APD restitution curve was computed to determine the DIs for which the slopes of restitution were 1 or greater. A curve was fit to the restitution data using TableCurve 2D v5.01 and the first derivative of the fitted   function was obtained using the same software. To simulate changes in a particular ionic current, at the end of the computation for that specific ionic current, the computed value of the current was multiplied by a factor 0.5 to represent 50% decrease in current and by a factor of 1.5 to constitute a 50% increase in current. Two types of pacing sequences were used; one was a constant DI protocol and the other sequence was used to obtain the restitution of APD and CV curves using the standard protocol.

Chapter Four: Results

We paced the tissue such that the feedback protocol ensured that the DI was constant at the pacing site, i.e. at the first cell. During pacing at constant DI = 40 msec, the first cell where DI control was established did not exhibit alternans (figure 1B). Figure 1C shows that all activations were conducted and as expected, the cycle length for all cells for any particular beat was the same. Calculation of conduction velocities did not reveal any variation from beat to beat. Restitution curves obtained using the standard protocol from the last cell in the fiber revealed slopes of restitution ($\Delta APD/\Delta DI$) to be always > 1 for all trials when the DI was less than 50ms. In the constant DI trial from which data are shown in figure 1, the first occurrence of alternans (using the 8 msec threshold) was at cell 38 once the pacing was switched to constant DI. Figure 2 illustrates action potentials obtained at the pacing site (figure 2A, cell 1) and at the last site (figure 2B, cell 220), clearly showing alternans at the end of the fiber. Restitution of APD and restitution of conduction velocity curves were obtained using the S1S2 pacing protocol and are shown in figures 3A and 3B. Figure 4 shows a time-space plot of the transmembrane voltages from all cells during the entire 100 beat pacing with constant DI protocol. In figure 4, time is on the x-axis and the cell numbers are on the y-axis with cell number 1 on the top. In figure 4, blue color represents repolarized state of a cell and yellow represents the depolarized states, therefore, blue bands indicate DI while yellow bands indicate APD. An expanded view, in figure 4B, clearly shows alternation of DI and of APD which is more pronounced in the bottom half of the fiber.

Reduction of sodium current, I_{Na} by 50% decreased rate of change of voltage during early part of action potential, as expected (figure 5A) and affected conduction velocity as well (decrease from 0.783 mm/ms for baseline I_{Na} to 0.578 mm/ms(figure 5B)). Interestingly, when I_{Na} was decreased by half, alternans were observed at the pacing site where DI's preceding each activation were held constant. Figure 5C shows very small variation in DI at the pacing site, a

consequence of the feedback protocol. The figure shows changes in DI to be less than 2ms. However, figure 5D shows that when I_{Na} was decreased, alternans of APD occurred at the pacing site as well. The conduction delay (the duration for an activation to travel from cell 1 to cell 220) observed during this trial with reduced Ina was 78ms as compared to a delay of 57ms for the protocol with baseline I_{Na}. The increased delay translated in a decrease in CV from 0.783 mm/ms during baseline level of I_{Na} to 0.578 mm/ms with decreased I_{Na}. The standard pacing protocol used during reduced I_{Na} showed that the slopes of APD restitution curves were greater than one for DIs less than 60ms as compared to being greater than one for DIs less than 50 ms during baseline conditions.

An increase in sodium current, I_{Na}, by 50% increased dv/dt as expected (figure 6A). As in figure 5A, figure 6A shows the start of action potentials during baseline levels of I_{Na} and increased I_{Na} current. With increased sodium current, I_{Na}, conduction velocity increased by 17% (i.e. from 0.783 mm/msec to 0.913 mm/msec). Alternans were observed nearer to the pacing site, i.e. at cell 31, when I_{Na} was increased compared to baseline levels of I_{Na}, in which case alternans occurred at cell 38. The slope of restitution of APD, obtained using the S1S2 pacing protocol had slopes greater than one at DIs < 50ms similar to those observed during baseline levels of I_{Na}. Pronounced alternans of APD were observed during increased I_{Na} at cells distal to the pacing site (figure 6B).

With decrease in calcium current (I_{CaL}), as expected, the APDs decreased as seen from figure 7A. While there were large changes in APD upon decrease in I_{CaL}, the variation in conduction velocity was small (change from 0.783 mm/ms for baseline levels of I_{CaL} to 0.789 mm/ms with reduced I_{CaL} (change of 0.8%)). The mean values of DI at the pacing site (cell 1) where DI control was established was calculated to be 38 ms and was 49 ms at the end of the fiber (cell 220) with a variation of ± 1ms. The plot APD at the pacing site (cell 1, blue) and at the end of the fiber (cell 220, red) revealed the variation in APD to be less than 3ms at both the pacing site and at the end of the fiber (figure 7B). Interestingly, APD

restitution curves revealed a linear relationship between APD and DI (figure 7C), with a slope of 0.24. Increase in calcium current (I_{CaL}), as expected, increased action potential duration (figure 8A) but did not have appreciable variation in conduction velocity as compared to baseline I_{CaL}, the change was only 0.15%.

When calcium current (I_{CaL}) was increased, alternans were not only absent at the pacing site but were also eliminated at the end of the fiber (figure 8B). The slope of the restitution of APD curve obtained for this ionic modification revealed slopes greater than 1 for DIs smaller than 41ms (figure 8C) although no alternans were observed.

To explore effects of cell to cell coupling in the genesis of alternans, the diffusion co-efficient (D_x) was reduced by 50%. The reduction in diffusion co-efficient resulted in slowing of conduction by 36% (change in CV from 0.783 mm/ms during baseline value to 0.5 mm/ms). No appreciable variation in APD compared with baseline (0.34%) was observed. Slope of the restitution of APD curve was greater than 1 for DIs less than 50ms similar to that seen during baseline values of the diffusion coefficient. With reduced diffusion coefficient, alternans were first observed at cell 20 in the fiber.

A decrease in potassium current (I_{kr}) resulted in an increase in APD when compared with baseline levels of I_{kr} (figure 9A), but conduction velocity was almost unaltered. The conduction velocity computed was 0.786 mm/ms as compared to 0.783 mm/ms for baseline levels of I_{kr}. Slope of restitution of APD became greater than 1 for DIs of 44ms and less. The first onset of alternans occurred at cell 65 in the fiber. Figure 9B, illustrates the APDs measured from cell one and cell 220. Though the variation in APD from beat to beat was not more than 1 ms at the pacing site (cell 1), variation in APD was as high as 32ms from beat to beat at cell 220.

An increase in the potassium current (I_{kr}) resulted in APD to be shortened (figure 10 A), and as with the case of decreased I_{kr}, no large variations in conduction velocity were detected (change of 0.2%). Slope of restitution of APD was greater than 1 for DIs less than 50ms similar to that observed during baseline values of I_{kr}. Alternans were first observed at cell 25 but were absent at the pacing site (figure 10 B). Figure 11 illustrates the summary of all ionic modifications that were executed and the cell number at which alternans first occurred for that ionic modification.
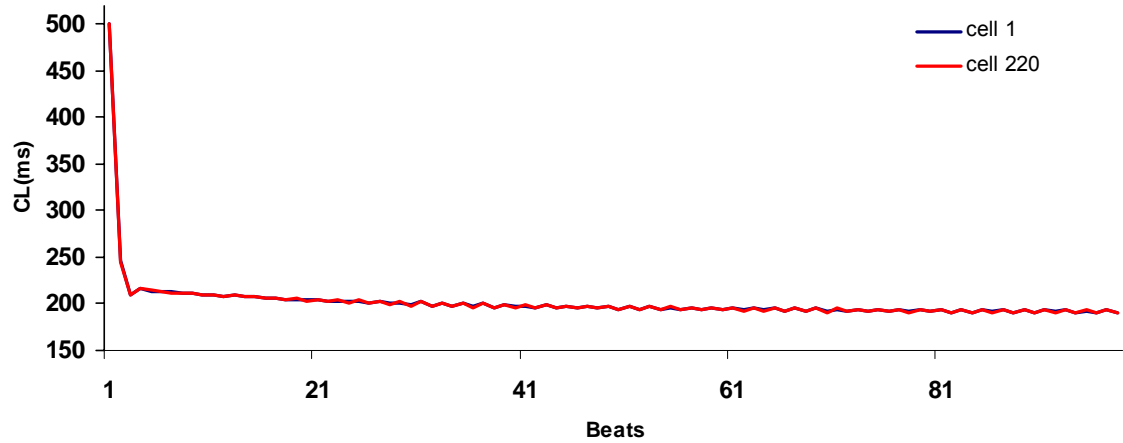
A
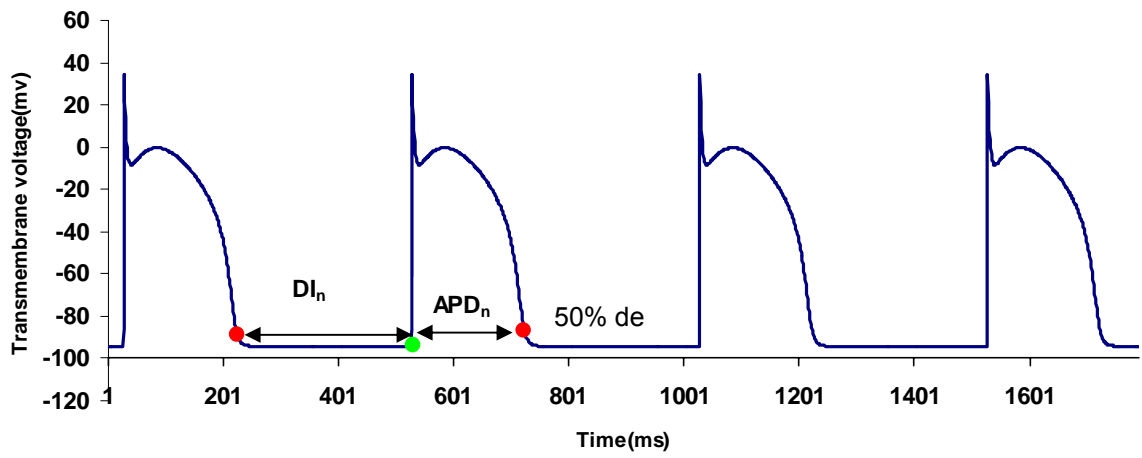
B
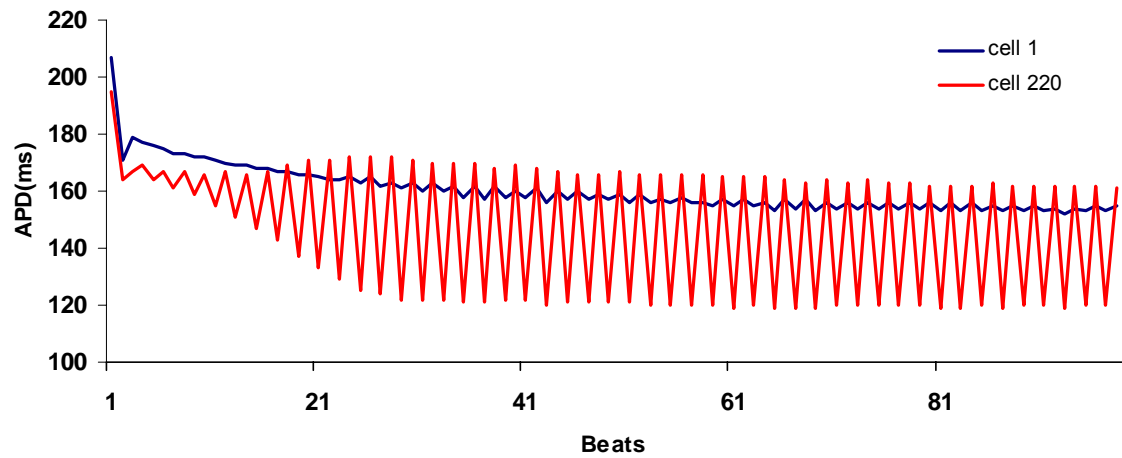
C

Figure 1A, illustrates the action potentials obtained from a single site paced at 500ms cycle length. Green circles indicate the start of the action potential while red circles represent 90 % of the action potential duration (APD$_{90}$). The points were determined by custom written programs. Figure 1B shows the beat to beat variation in APD. Cell 1(blue) did not reveal any APD alternans whereas alternans were very prominent at cell 220(red). Cell one APD characteristics also reveals the progressive decrease in APD with time until a steady state is reached. Figure 1C. Progressive decrease in cycle length CL as pacing protocol is switched from constant cycle length pacing to constant DI pacing with DI= 40ms. Note that cycle length of cell 1(blue) and cell 220(red) are identical.

13

A
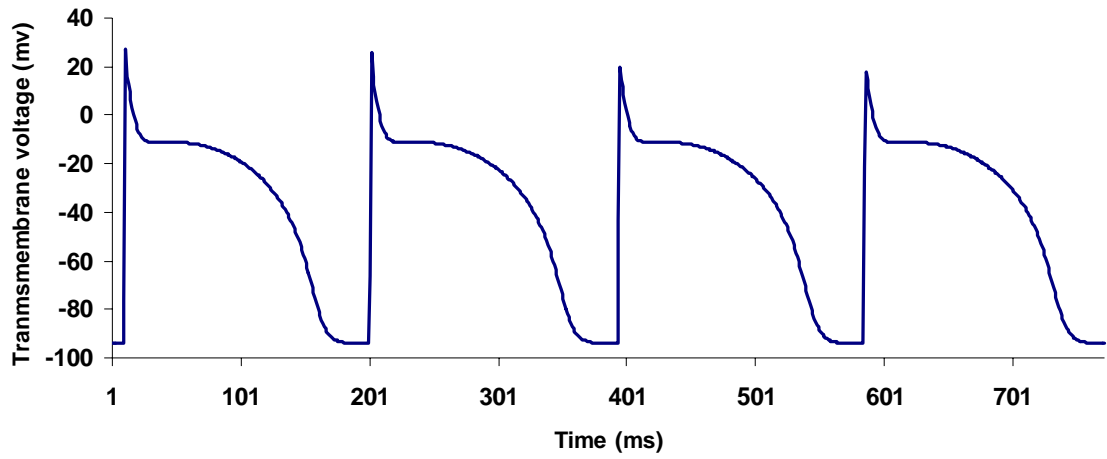
B

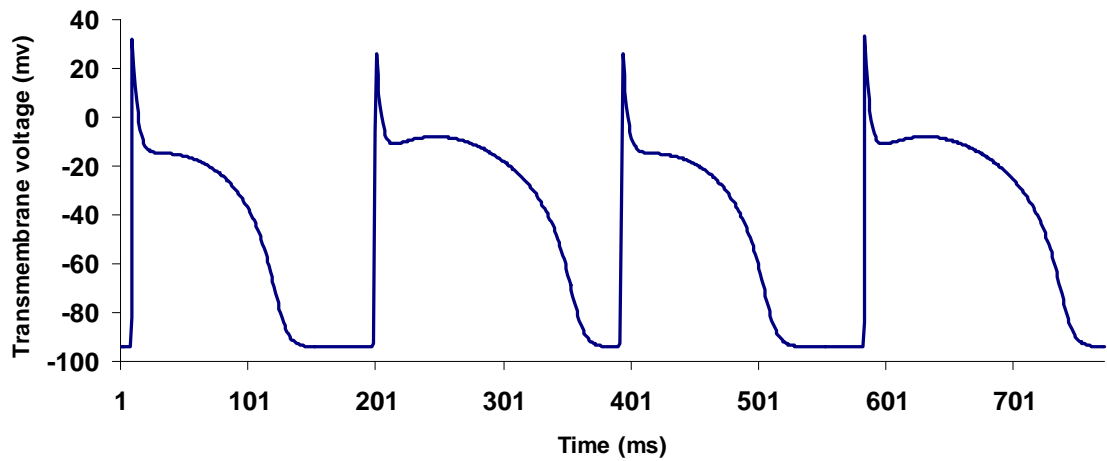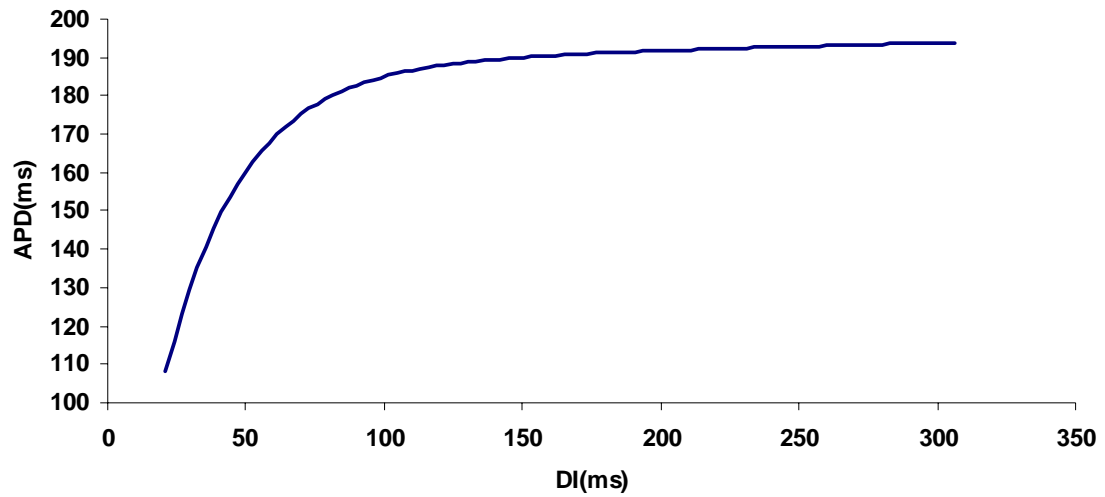Figure 2. Plot of action potentials of A, cell 1 and B, cell 220 at the end of the simulation reveals presence of alternans in cell 220 but not in cell 1. Alternans were first observed at cell 38.

A

B
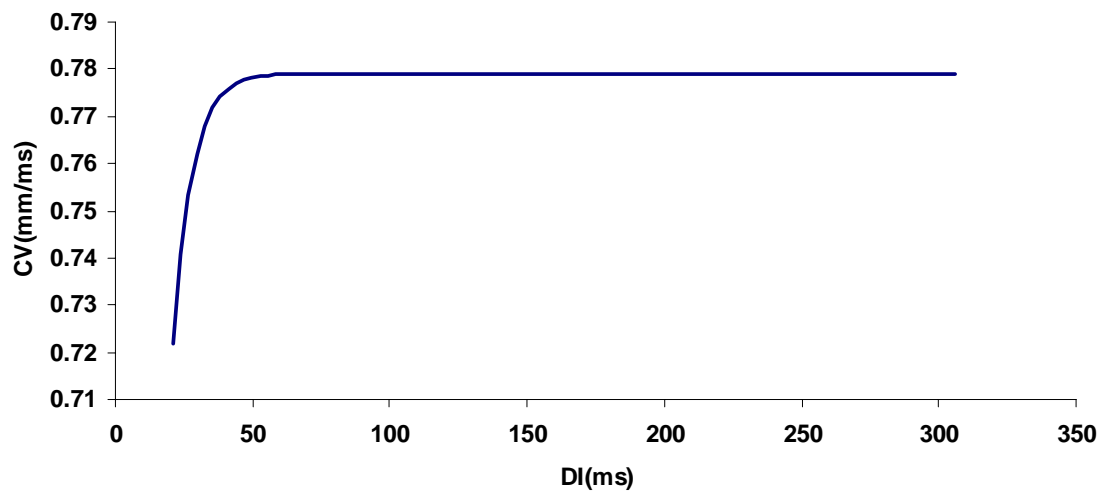
Figure 3A and 3B shows the restitution of APD (from cell 220) and restitution of CV obtained using the S1S2 pacing protocol. Curve fitting was done using the software Tablecurve 2D, SYSTAT software Inc.

15

A
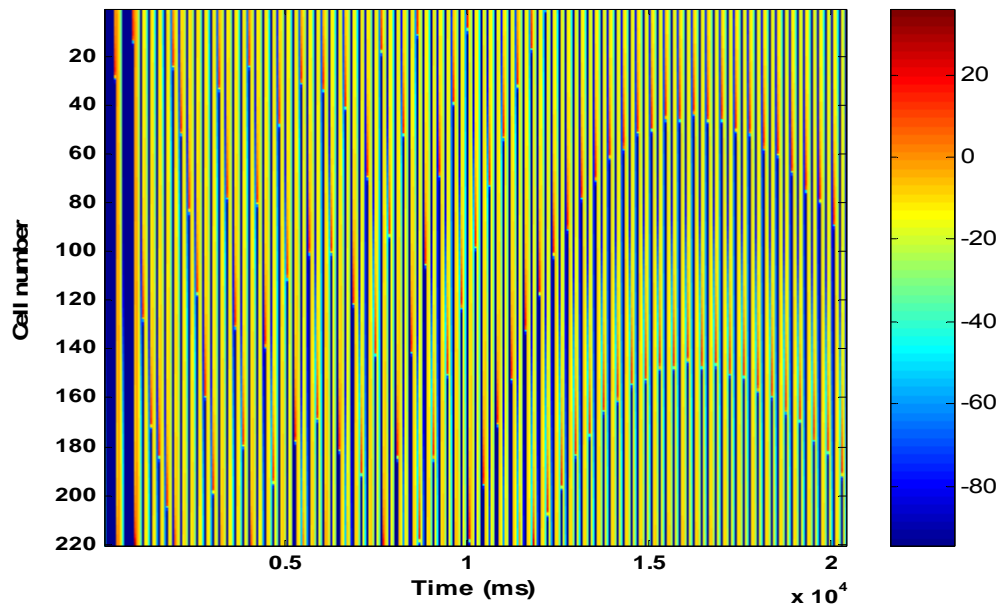
B
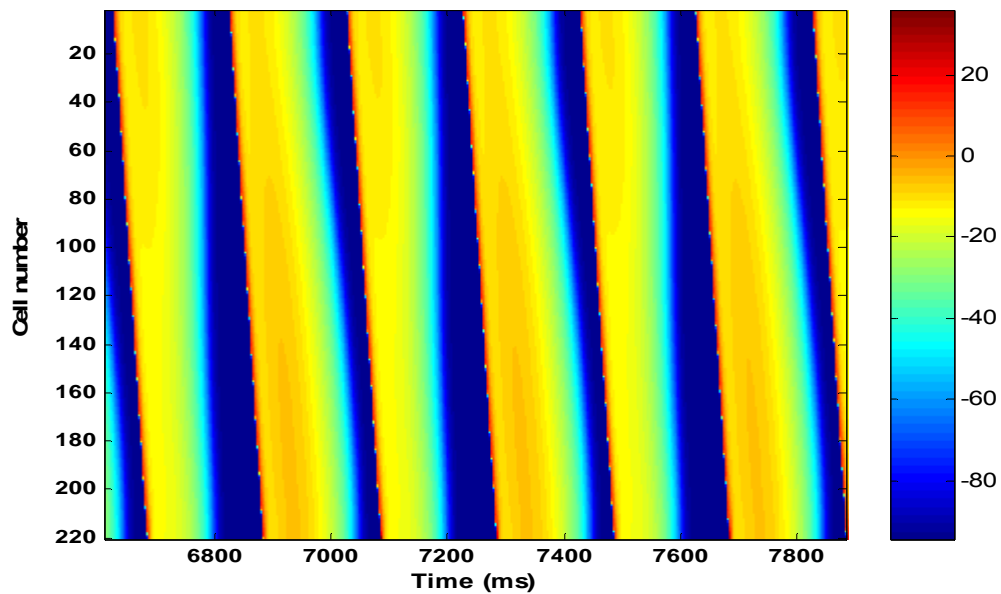
Figure 4A Two dimensional map obtained with time (ms) on the x-axis and cell number on the y-axis. The blue shades are representative of DI while the yellow shades are representative of action potential duration. An expanded view, in figure 4B clearly reveals alternation in DI and of APD. The color legend represents the value of the transmembrane voltage.

A
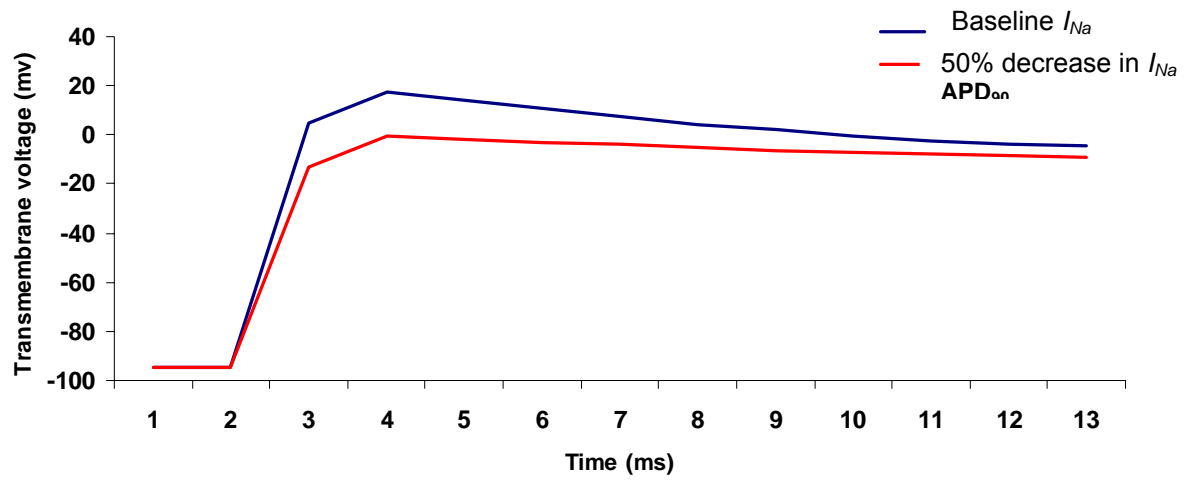
B
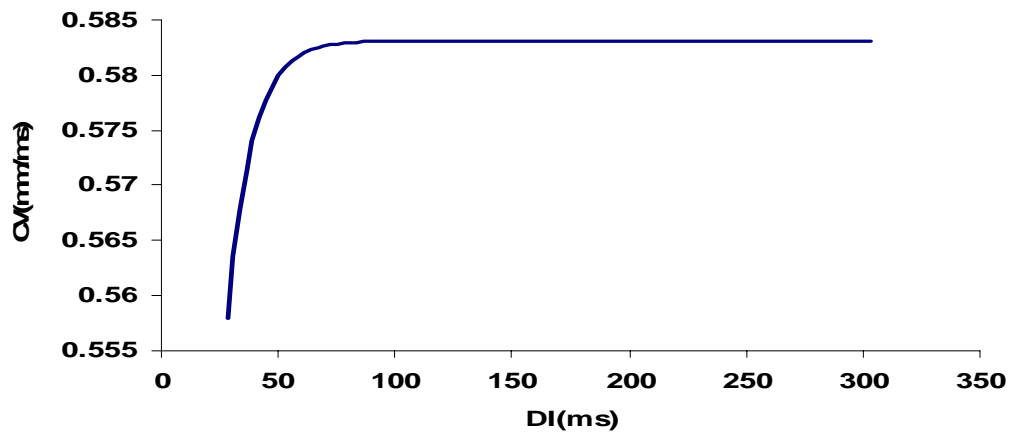
C
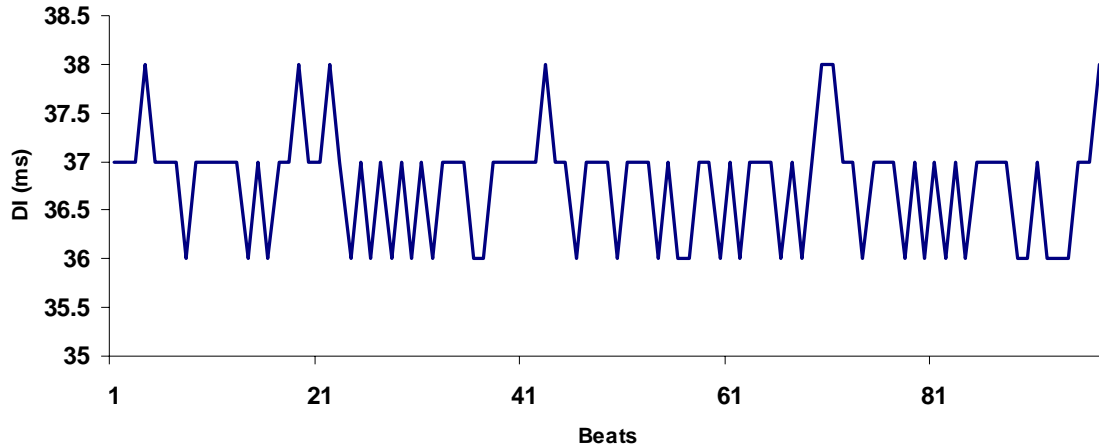
D
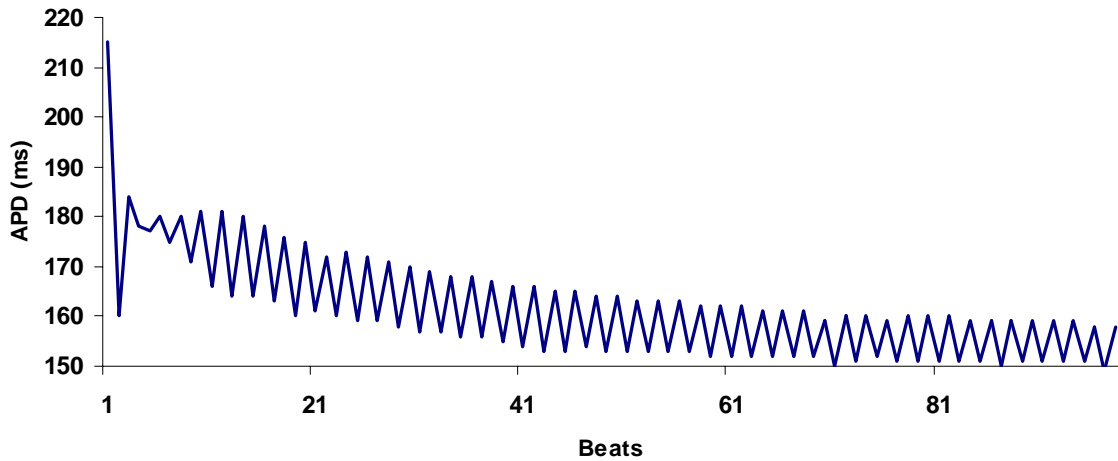
Figure 5A shows the start of action potentials during baseline (blue) and reduced sodium current conditions (red) that exhibits lower dv/dt when sodium current (I_{Na}) is reduced. Figure 5B. Restitution of CV exhibits lower conduction velocity for reduced I_{Na} when compared with baseline levels of I_{Na} (figure 3B). Figure 5C. With decreased I_{Na}, alternation in DI at the pacing site (cell 1) was small (≤2ms), however, alternans of APD were evident at the pacing site (figure 5D).

A

B
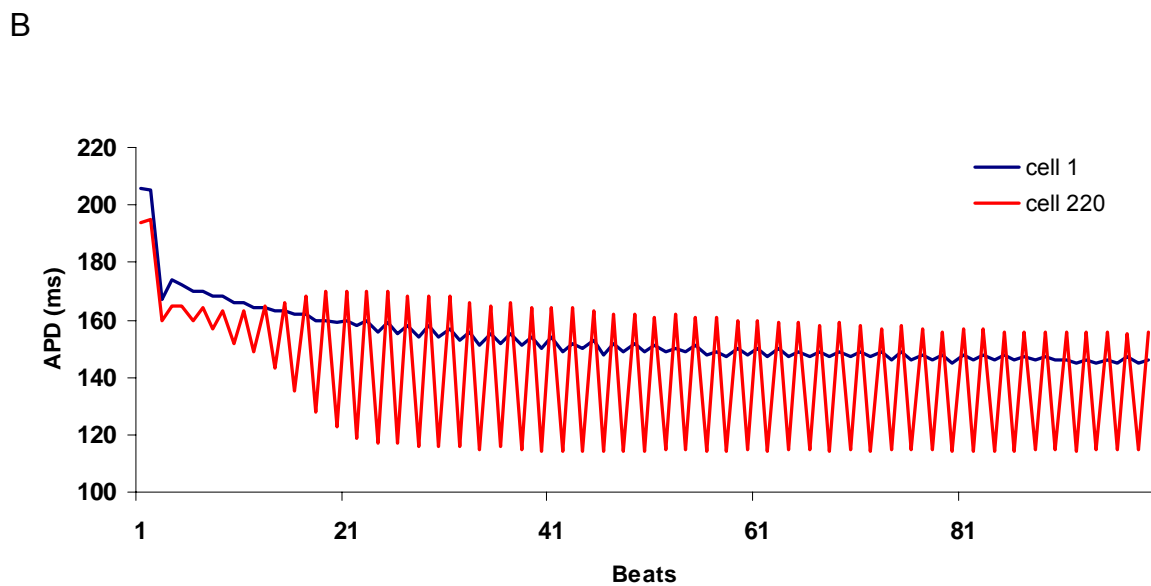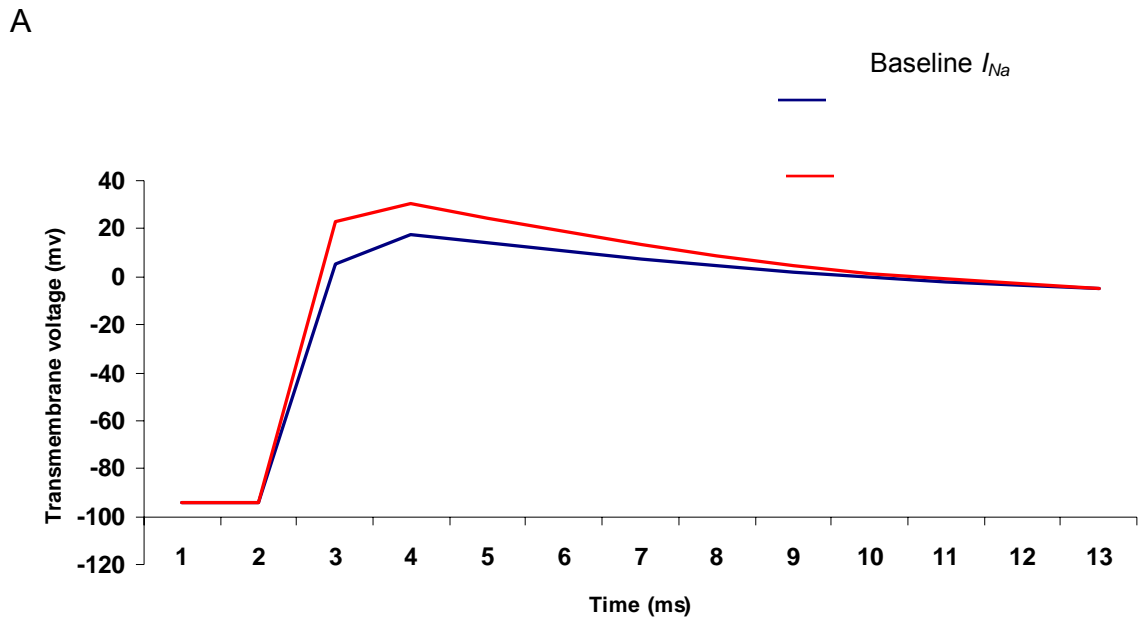
Figure 6A shows the start of action potentials during baseline (blue) and increased sodium current conditions (red) that exhibits higher dv/dt when sodium current (I_{Na}) is increased by 50%. Figure 6B. With increased I_{Na} , alternation in APD at the pacing site (blue, cell 1) was small (≤4ms), however, alternans of APD at the end of the fiber (red, cell 220) was as high as 45ms (figure 6B).

A
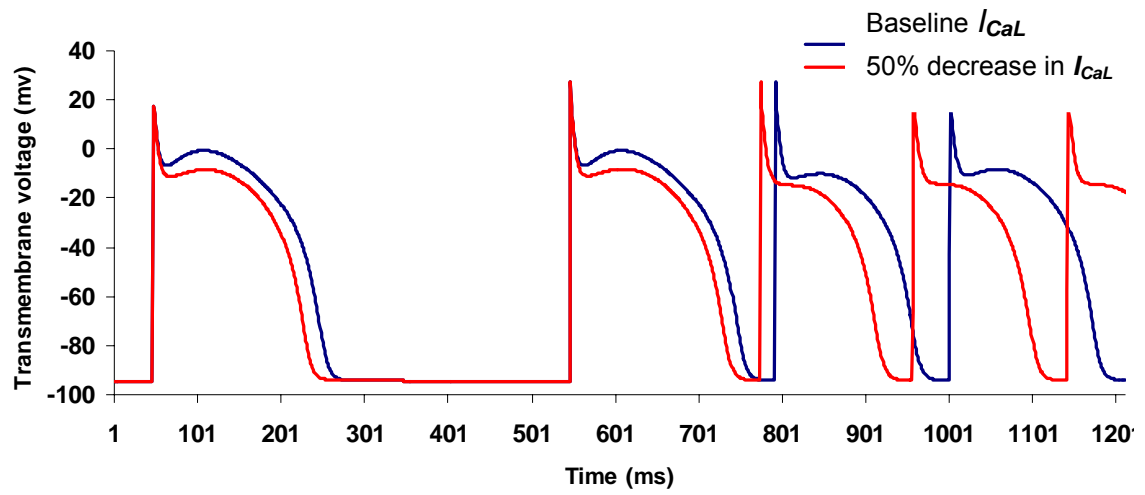
B
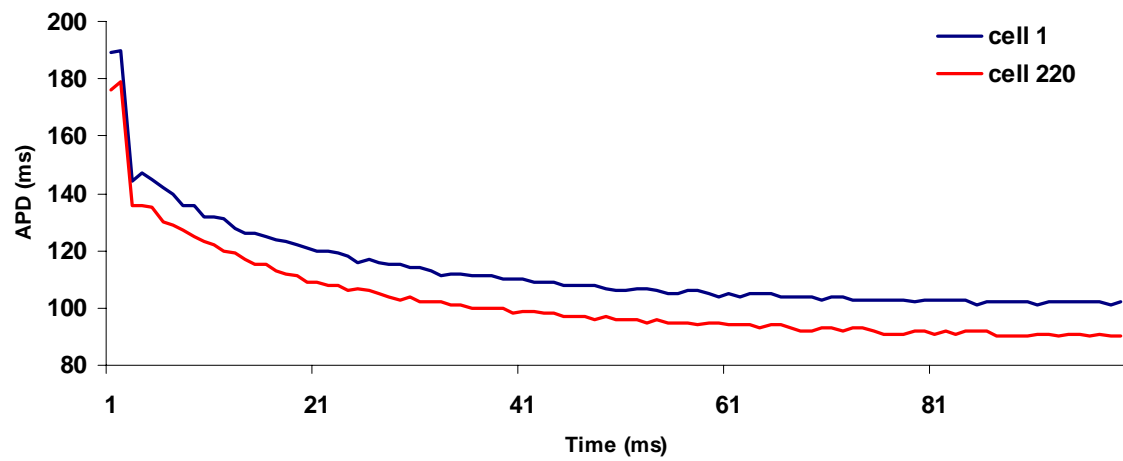
C
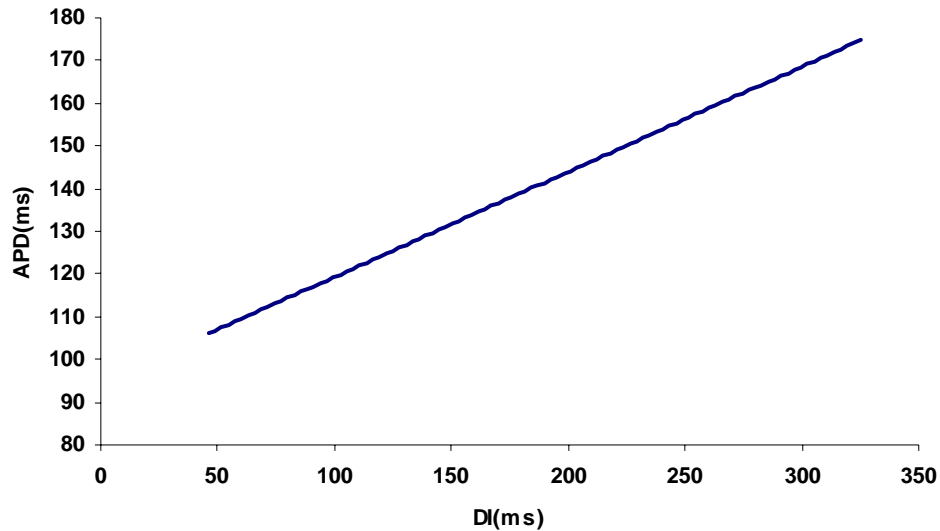
Figure 7A. Reduction of APD evident with reduced calcium current (I_{CaL}, red) The trace shows the last two beats of constant cycle length pacing followed by the first three beats at constant DI pacing with DI= 40ms. Figure 7B. The variation in APD at the pacing site (cell 1, blue) and at cell 220(red) was very small (≤3ms). Figure 7C. Restitution of APD at cell 220 obtained using S1S2 pacing protocol revealed a linear relationship between APD and DI. The slope was constant at 0.24. Curve fitting was done using the software, Tablecurve 2D, SYSTAT software Inc.

21

A
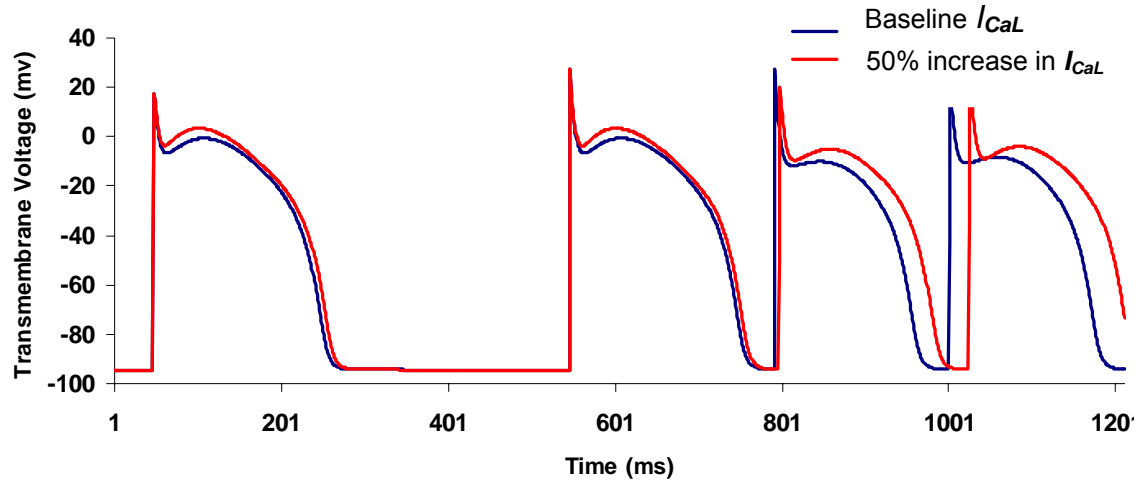
B
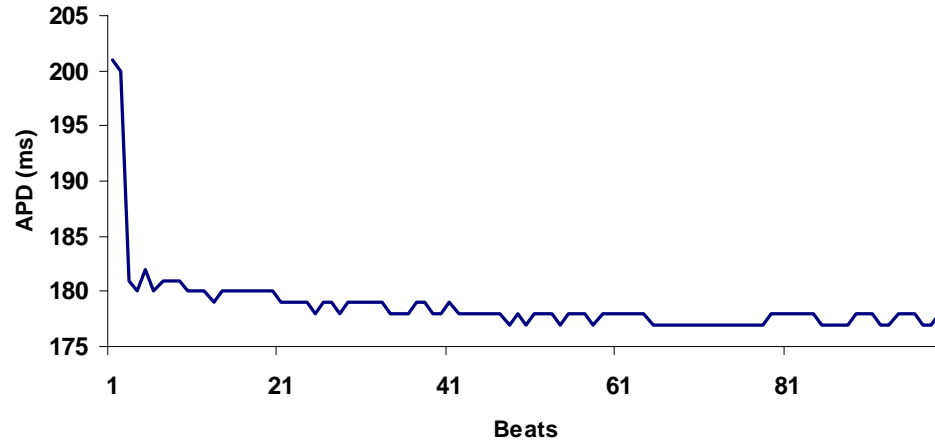
C
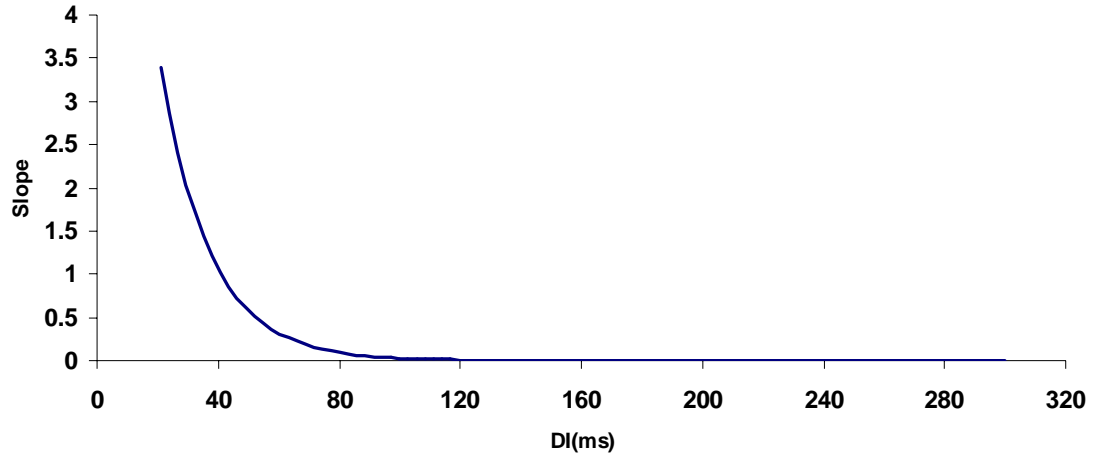
Figure 8A. Elevation in APD with calcium current, I_{CaL} enhanced by 50% (red) when compared with baseline I_{CaL} (blue). The trace shows the last two beats of constant cycle length pacing followed by the first three beats at constant DI pacing with DI= 40ms. Figure 8B. When calcium current was increased, the beat by beat change in APD observed at cell 220 was very small (≤3ms). Figure 8C. Slope of restitution of action potential duration for enhanced calcium current, I_{CaL} using the S1S2 pacing protocol. The slope of the curve fitted data was obtained using the software Tablecurve 2D, SYSTAT software Inc.

23

A
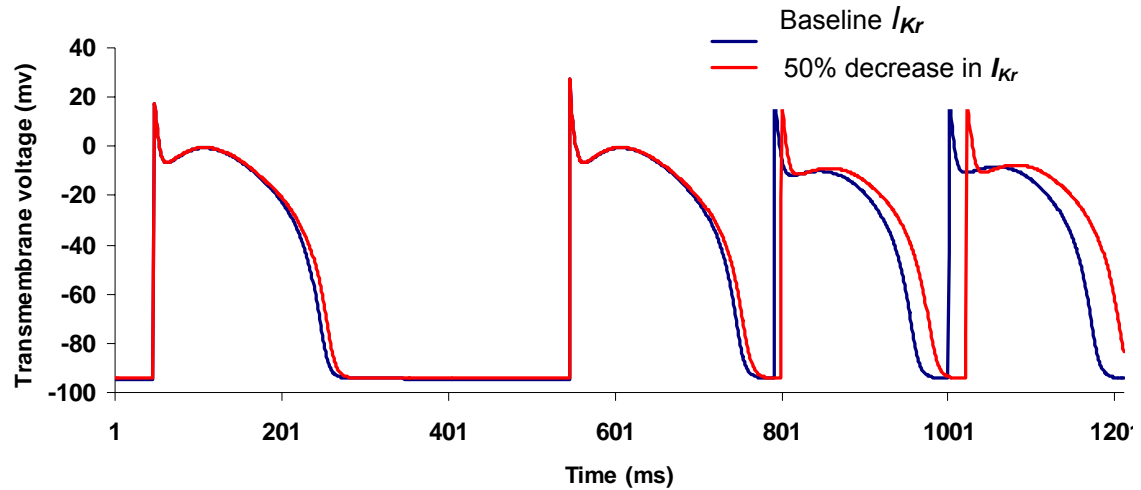
B
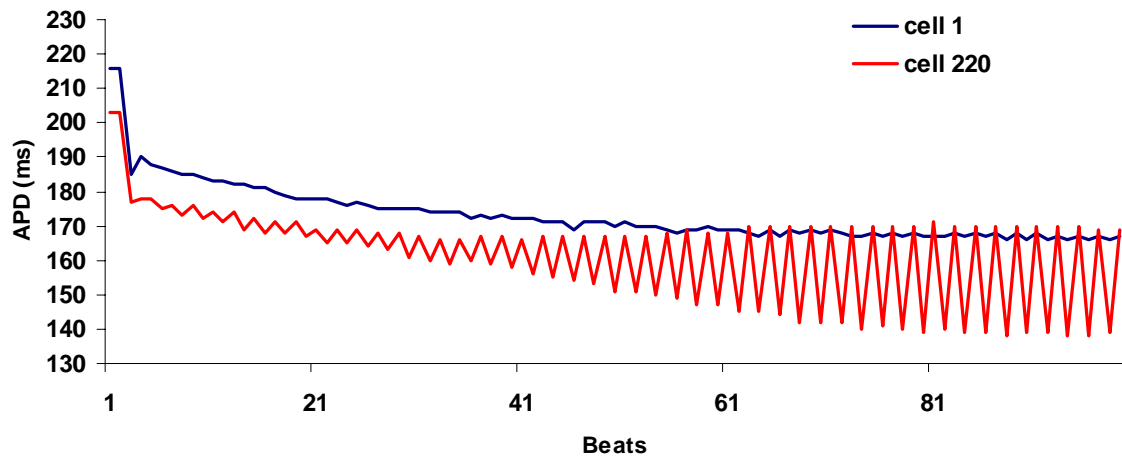
Figure 9A. Elevation in APD with potassium current, I_{Kr} decreased by 50% (red) when compared with baseline I_{Kr} (blue). The trace shows the last two beats of constant cycle length pacing followed by the first two beats at constant DI pacing with DI= 40ms. Figure 9B. With decreased I_{Kr}, the beat by beat change in APD observed at the pacing site (cell 1, blue) was very small (≤2ms) although alternation in APD at the last cell (cell 220, red) was as high as 32 ms.

24

A
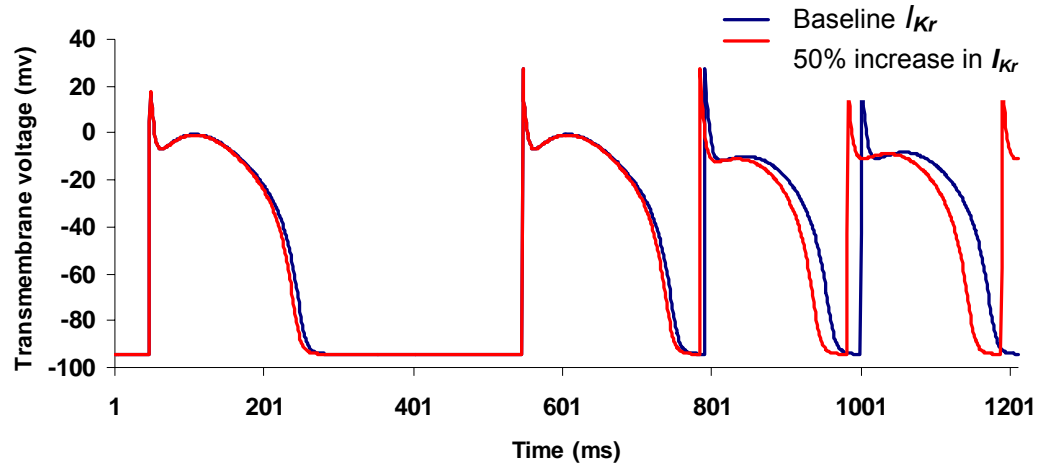
B
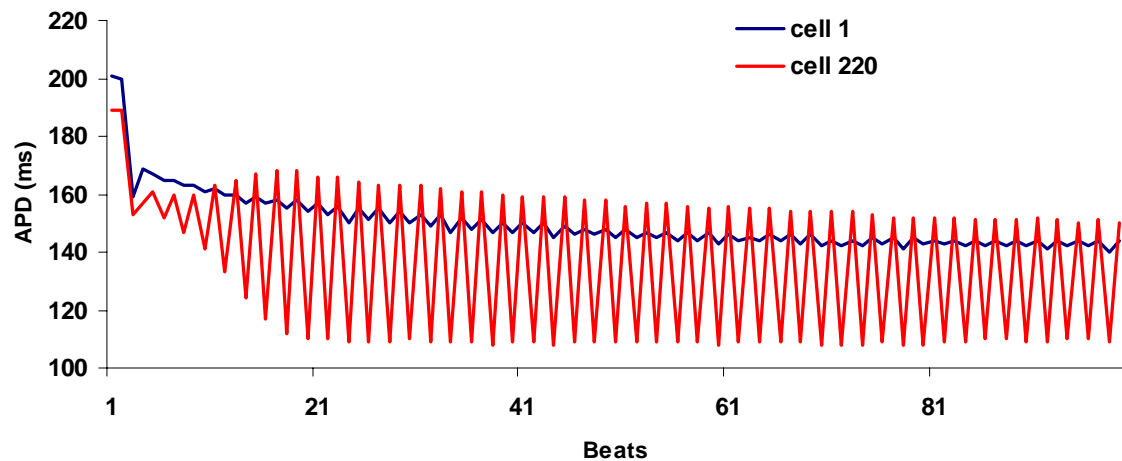
Figure 10A. Decrease in APD with potassium current, I_{Kr} increased by 50% (red) when compared with baseline I_{Kr} (blue). The trace shows the last two beats of constant cycle length pacing followed by the first two beats at constant DI pacing with DI= 40ms. Figure 10B. With increased I_{Kr}, the beat by beat change in APD observed at the pacing site (cell 1, blue) was very small (≤2ms) although alternation in APD at the last cell (cell 220, red) was as high as 56 ms.
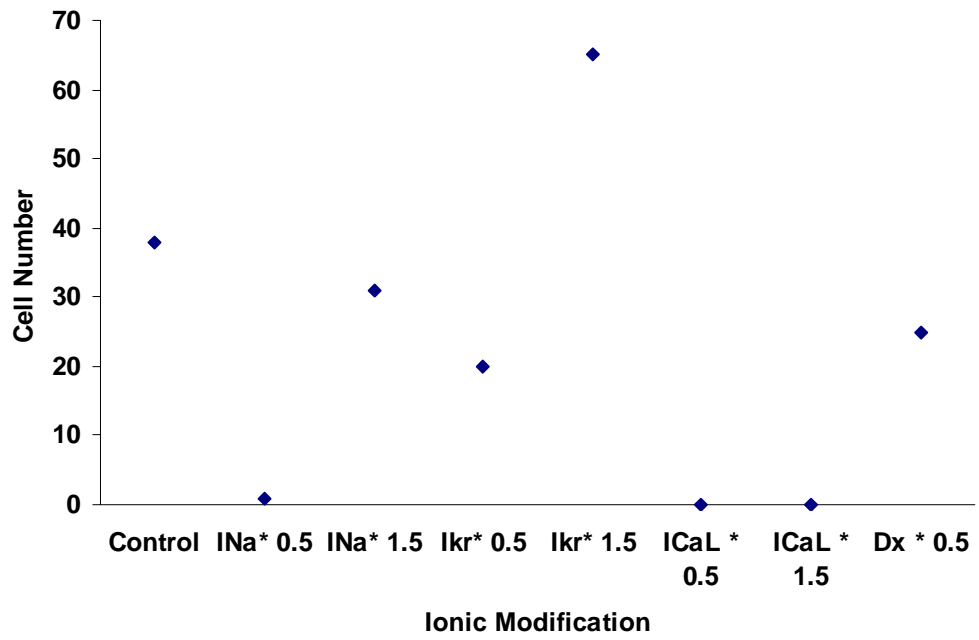
Figure 11. Summary of all ionic modifications that were executed and the cell number at which alternans first occurred for that ionic modification.

Chapter Five: Discussion

Our main objective in this study was to explore mechanisms of alternans of APD that occur in a one dimensional fiber when pacing is initiated at one end of the fiber such that DI's preceding each activation at the paced site are invariant. The reason for removing changes in DI at the pacing site was that this eliminated a confound of restitution of APD at the site of origin of activation that is present in virtually all previous investigations of effects of spatio-temporal parameters on alternans of APD.

We observed that even when alternans of APD were eliminated at the pacing site via use of DI control, alternans occurred downstream in the fiber in the model with nominal parameters (i.e. in normal state). A possible mechanism of the occurrence of alternans in this circumstance is as follows: When pacing was switched to shorter DIs during DI control, the cycle lengths decreased progressively because of slower adaptation of APDs until they reached a steady state (figure 1C). This phenomenon of slow adaptation of APD to a decreased cycle length of pacing has been seen in previous studies [38]. After switching to constant DI, the APD of the cell at the pacing site shortened compared to the previous APD because of shorter DI as a result of restitution of APD as shown by Pt. 1 in figure 11, 172 ms compared to previous APD of 207ms). There was a 57±1 ms delay for the depolarization to travel from the first cell to the last cell (figure 11, Pt.2). The DI was maintained nearly constant (note the very small variation in DI at the pacing site) at 40 ms at the pacing site (cell 1) but because of constant conduction delay (56 ms) and shorter APDs for cells away from the pacing site the DI for the last cell became 51ms (figure 11, Pt.3). The APD was longest at the pacing site but decreased down the fiber. The likely reason for increased APD being that the stimulus current was added only at the pacing site (cell number 1) at the predetermined DI and the charge was distributed down the fiber because of the diffusive process. At the pacing site for the next beat, the DI being constant and the cycle length being progressively shortened, the

depolarization charge at the last cell arrived at an earlier time (i.e. DI was shortened, equal to 45 ms, figure 11, Pt.4) compared to the previous DI of 51ms.

The decrease in DI was because conduction delay was almost constant. As a consequence of short DI, the succeeding APD became shorter compared to the previous APD. The cycle length being constant, the DI for the next beat at the last cell became longer than the previous beat producing a longer APD. This cycle was repetitive and the difference between the DI's of one beat to the other beat progressively increased (figure 12) as the cycle length at the pacing site and at all other sites progressively decreased (figure 13). Figure 13 which is an expanded view of figure 1C, shows the progressive decrease in CL with constant DI pacing accompanied by slight alternation in CL. The alternation in CL was not more than 3ms although alternations in APD of 40ms were observed in the last cell (cell 220).

We explored effects of changes in sodium current, I_{Na} because of its role in conduction. A decrease in sodium current caused alternans to occur at the pacing site. In a previous study by others in which a single cell was simulated, reduction of Ina was reported to increase the magnitude of alternans but the simulation was done using cycle length pacing [33]. However when we recreated the same model of the single cell and used a DI based feedback protocol no alternans were observed even for very short DIs including a 0ms DI. Using the same mechanism that we propose above explains the mechanism of alternans during the DI control protocol, with decreased I_{Na} alternans were expected to occur earlier in the fiber as the APDs were similar to that during baseline I_{Na} but the conduction delay was much higher, subsequently the DI for the last cell increased. The APDs however decreased until they approached a steady value. The increase in conduction delay caused the difference between the consecutive DI's for the same cell to increase. However, reasons as to why alternans occurred at the pacing site still remain unclear. Increased I_{Na} would cause alternans to occur nearer to the pacing site in the fiber as there was an increase

28

in conduction velocity but the difference between successive DIs was similar to baseline I_{Na}.

It can be concluded from the two modifications of decreasing and increasing I_{Na} that slowing of conduction has a greater influence in the genesis of alternans than increasing conduction velocity.

Calcium current, I_{CaL} plays a major role in the plateau phase of the action potential and hence has a major influence on the APD. I_{CaL} has also been reported to dramatically affect the slope of the restitution curve[39]. In our study, elevation or decrease in I_{CaL} had the same response of eliminating alternans. Even though restitution slope was less than one (0.24) with reduction of I_{CaL} and resulted in no alternans, alternans were eliminated when the slope of the APD restitution was equal or greater than one for the region of pacing with increased I_{CaL} contrary to what the restitution hypothesis would suggest for the value of the slope for alternans to occur. Elimination of alternans by blocking the calcium current, I_{CaL}, would require the use of I_{CaL} blocker clinically, unfortunately, the disadvantage of using calcium channel blockers clinically is that it would result in reduction of contractile force [33].

Reduction of the diffusion co-efficient is similar to gap junctional uncoupling and as expected the reduction of the diffusion co-efficient by half slowed conduction[40]. Although reduced diffusion caused conduction velocity to be much lower than during baseline, the APDs were similar to the baseline protocol. The reduction in diffusion caused an increased conduction delay, increasing the DI for the last cell much more than the baseline diffusion co-efficient and hence an increase between the successive difference in DIs for the last cell. We consider that the increase in successive differences between the DIs was the reason alternans occurred nearer to the pacing site in the fiber (cell 20).

Potassium currents, like calcium currents, also have a direct influence on the APD. An elevation in potassium current would reduce the APD whereas a decrease would increase the APD. With respect to the mechanism of alternans, during changes in potassium current (I_{kr}), similar conduction velocities (between baseline and decreased I_{kr}) and an increase in APD resulted in successive differences between the consecutive DIs to become smaller. This decrease in the difference in DI resulted in alternans to occur farther away from the pacing site in the fiber, i.e. at cell 65. For the protocol with increased I_{kr}, similar conduction velocities, but with decreased APDs compared to the baseline levels of I_{kr}, resulted in alternans occurring earlier in the fiber (cell 25). Fox et al [33] had reported the elimination of alternans with a 62% increase in I_{kr} in a single cell model. Even with 65% increase in I_{kr}, alternans were not eliminated in our model. In his single cell model, Fox et al [33] had also reported the elimination of alternans with increase in the transient outward K^+, I_{to} and the inward rectifier K^+, I_{K1} current. We however did not observe similar results. The differences may be attributed to the fact that cells in isolation can behave differently electrically than cells that are inter-linked together in the tissue [41].

Effects of change in sodium conductance (g_{Na}) and its influence on the calcium current (I_{CaL}) or the effects of sodium current (I_{Na}) on the calcium current (I_{CaL}) was not studied.

30
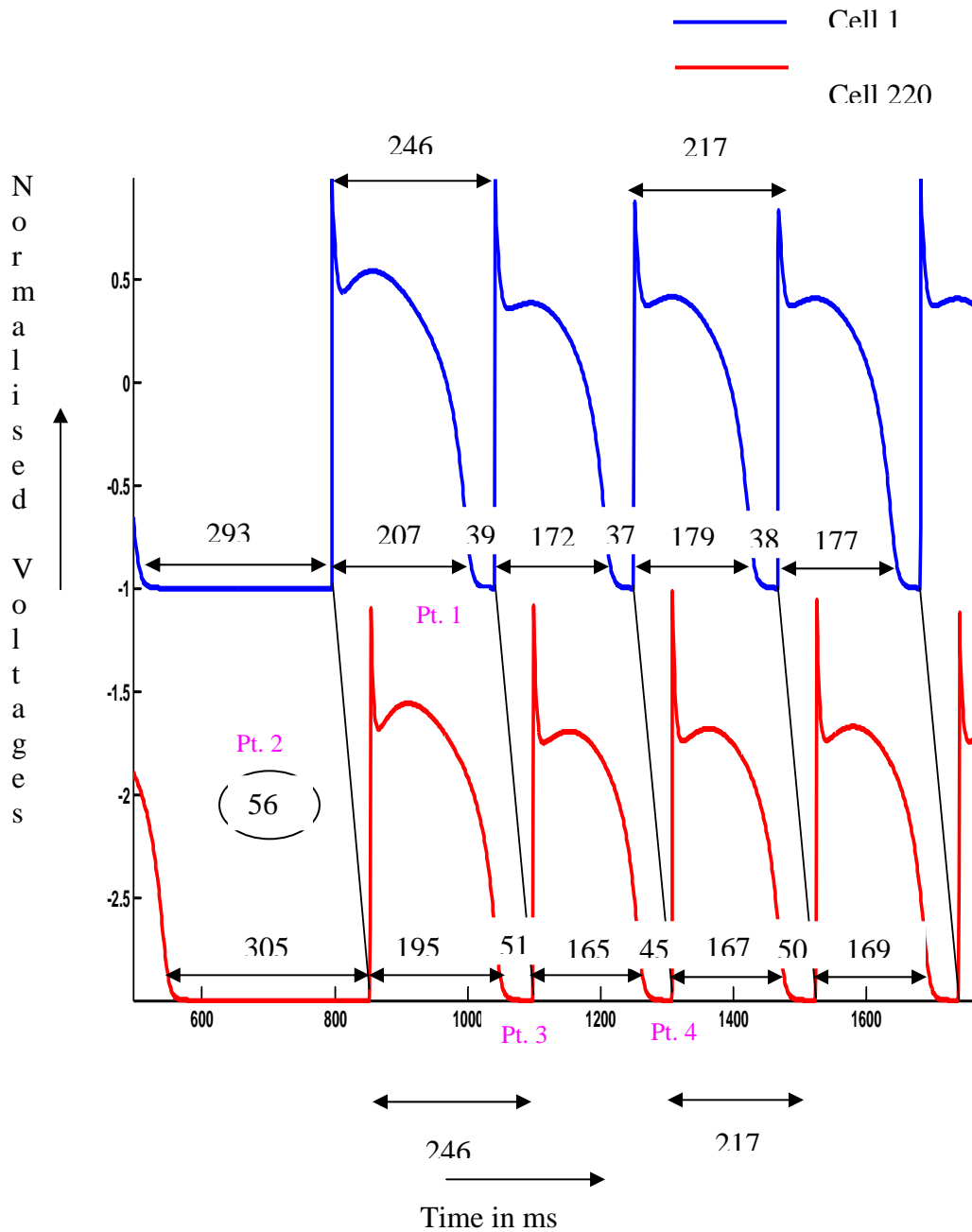
Figure 12. Plot of transmembrane voltages (normalized) at the pacing site (cell 1, blue) and at the end of the fiber (cell 220, red). All values in the figure except for the normalized values in the y-axis have units in milliseconds. Illustrated is the last beat of constant cycle length pacing (500ms) followed by constant DI pacing through feedback control at 40ms at the pacing site.
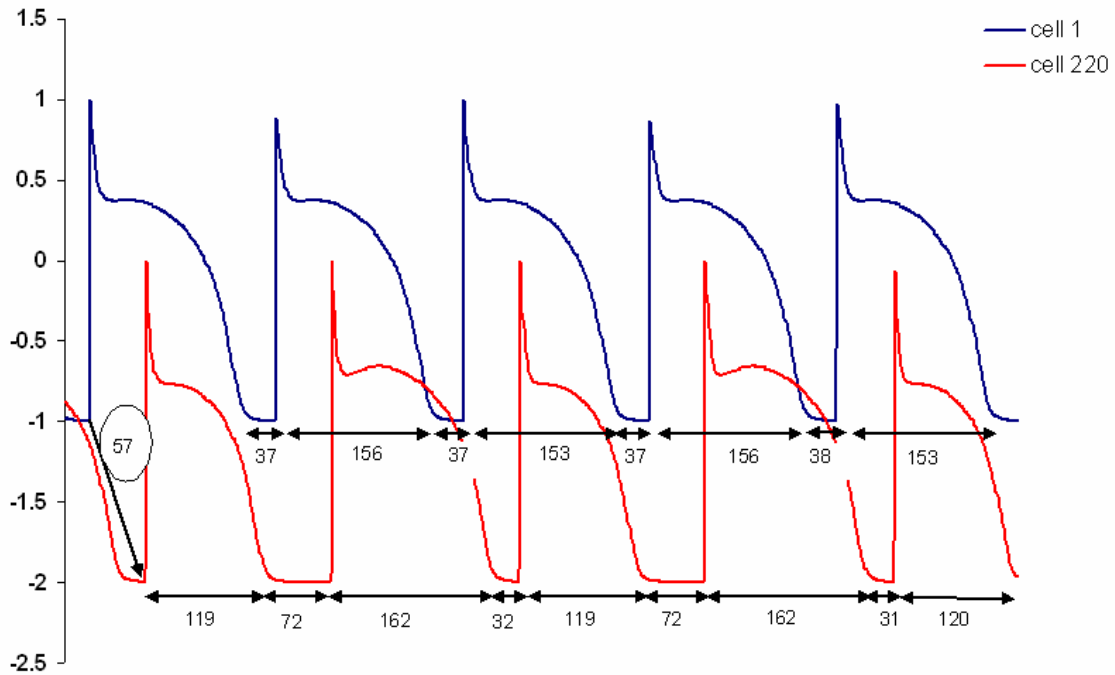
Figure 13. Plot of transmembrane voltages (normalized) at the pacing site (cell 1, blue) and at the end of the fiber (cell 220, red). All values in the figure except for the normalized values in the y-axis have units in milliseconds. Illustrated are action potentials at beats 80-84 to show the increase in alternation of DI and of APD at the end of the fiber (cell 220, red) with time.
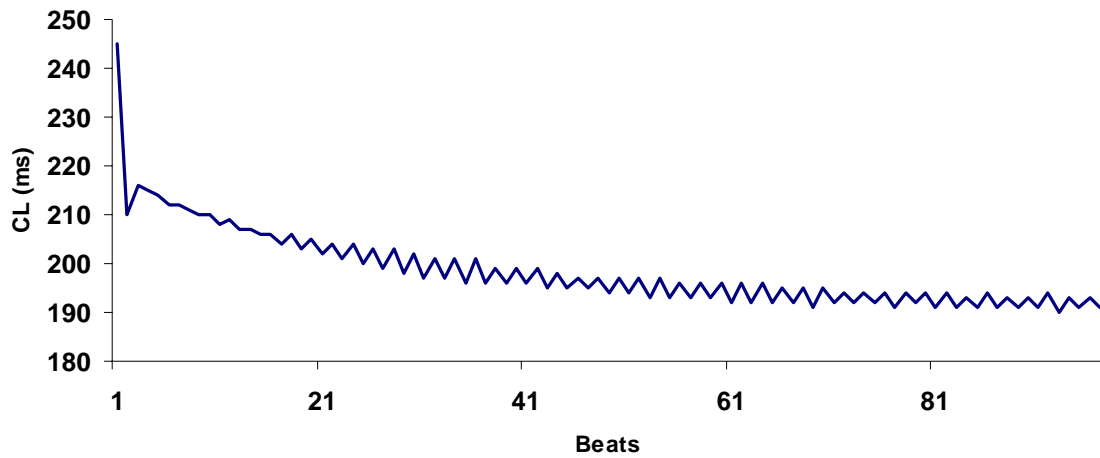
Figure 14. Progressive decrease in cycle length with constant DI (40 ms) at cell 220. All cells had the same cycle length (figure 1C). Alternations in CL was not more than 3ms.

Chapter Six: Limitations

The major limitation of our study is that it is a simulation. Like all other models it suffers from various limitations. One such limitation is the way in which calcium is handled. Most models like the CVM model correspond to an all or none response whereas global rise in calcium is due to the summation of many local release events or calcium sparks [42-46]. Coupled to the above limitation is that there is no separate handling for the junctional sarcoplasmic reticulum in the CVM as the concentrations of calcium in the JSR and NSR have been combined to a single variable. This is because there is evidence to suggest that local depletion of JSR plays an important role in spark termination [47, 48]. The model being a one dimensional model would not be physiologically very relevant as there is evidence to show that a single cell is coupled to 11± 2 other cells [49].

References

1. Roth, B.J., The pinwheel experiment revisited. J Theor Biol, 1998. 190(4): p. 389-93.

2. Shibata, N., et al., Influence of shock strength and timing on induction of ventricular arrhythmias in dogs. Am J Physiol, 1988. 255(4 Pt 2): p. H891-901.

3. Chen, P.S., et al., Mechanism of ventricular vulnerability to single premature stimuli in open-chest dogs. Circ Res, 1988. 62(6): p. 1191-209.

4. Winfree, A.T., Electrical instability in cardiac muscle: phase singularities and rotors. J Theor Biol, 1989. 138(3): p. 353-405.

5. Qu, Z., A. Garfinkel, and J.N. Weiss, Vulnerable window for conduction block in a one-dimensional cable of cardiac cells, 1: single extrasystoles. Biophys J, 2006. 91(3): p. 793-804.

6. Fox, J.J., et al., Spatiotemporal transition to conduction block in canine ventricle. Circ Res, 2002. 90(3): p. 289-96.

7. Weiss, J.N., et al., Chaos and the transition to ventricular fibrillation: a new approach to antiarrhythmic drug evaluation. Circulation, 1999. 99(21): p. 2819-26.

8. Riccio, M.L., M.L. Koller, and R.F. Gilmour, Jr., Electrical restitution and spatiotemporal organization during ventricular fibrillation. Circ Res, 1999. 84(8): p. 955-63.

9. Garfinkel, A., et al., Preventing ventricular fibrillation by flattening cardiac restitution. Proc Natl Acad Sci U S A, 2000. 97(11): p. 6061-6.

10. Wu, R. and A. Patwardhan, Mechanism of repolarization alternans has restitution of action potential duration dependent and independent components. J Cardiovasc Electrophysiol, 2006. 17(1): p. 87-93.

11. Fenton, F.H., et al., Multiple mechanisms of spiral wave breakup in a model of cardiac electrical activity. Chaos, 2002. 12(3): p. 852-892.

12. Draper, M.H. and M. Mya-Tu, A comparison of the conduction velocity in cardiac tissues of various mammals. Q J Exp Physiol Cogn Med Sci, 1959. 44(1): p. 91-109.

13. Patwardhan, A. and S. Moghe, Novel feedback based stimulation protocol shows hysteresis in cardiac action potential duration restitution. Biomed Sci Instrum, 2001. 37: p. 505-10.

14. Eric P. Widmaier, H.R., Kevin T. Strang, Vander, Sherman, Luciano's Human Physiology : the mechanisms of body function NINTH EDITION ed.

15. Sudden Cardiac death: American Heart Association, 2007 [cited; Available from: http://www.americanheart.org/presenter.jhtml?identifier=4741

16. Ventricular Fibrillation: American Heart Association, 2007 [cited; Available from: http://www.americanheart.org/presenter.jhtml?identifier=4784

17. Jalife, J., Ventricular fibrillation: mechanisms of initiation and maintenance. Annu Rev Physiol, 2000. 62: p. 25-50.

18. Zipes, D.P. and H.J. Wellens, Sudden cardiac death. Circulation, 1998. 98(21): p. 2334-51.

19. DP Zipes, J.J., Clinical and Experimental pathophysiology of sudden cardiac death, in Cardiac Electrophysiology: From Cell to Bedside 1990. p. 666-78.

20. DP Zipes, J.J., Ventricular Fibrillation, in Cardiac Electrophysiology: From Cell to Bedside 1995. p. 927-33.

21. DP Zipes, J.J., Three dimensional vortex-like reentry, in Cardiac Electrophysiology: From Cell to Bedside 1995. p. 403-10.

22. Gray, R.A., et al., Mechanisms of cardiac fibrillation. Science, 1995. 270(5239): p. 1222-3; author reply 1224-5.

23. Gray, R.A., A.M. Pertsov, and J. Jalife, Spatial and temporal organization during cardiac fibrillation. Nature, 1998. 392(6671): p. 75-8.

24. Marban, E., S.W. Robinson, and W.G. Wier, Mechanisms of arrhythmogenic delayed and early afterdepolarizations in ferret ventricular muscle. J Clin Invest, 1986. 78(5): p. 1185-92.

25. Rosen MR, G.H., Hoffman BF, Correlation between the effects of ouabain in the canine electrocardiogram and transmembrane potential of isolated purkinje fibers. circulation, 1973(47): p. 65-72.

26. Cao, J.M., et al., Spatiotemporal heterogeneity in the induction of ventricular fibrillation by rapid pacing: importance of cardiac restitution properties. Circ Res, 1999. 84(11): p. 1318-31.

27. Bass, B.G., Restitution of the action potential in cat papillary muscle. Am J Physiol, 1975. 228(6): p. 1717-24.

28. Koller, M.L., M.L. Riccio, and R.F. Gilmour, Jr., Dynamic restitution of action potential duration during electrical alternans and ventricular fibrillation. Am J Physiol, 1998. 275(5 Pt 2): p. H1635-42.

29. Nolasco, J.B. and R.W. Dahlen, A graphic method for the study of alternation in cardiac action potentials. J Appl Physiol, 1968. 25(2): p. 191-6.

30. Guevara MR, W.G., Shrier A, Giass L, Electrical alternans and period doubling bifurcations. IEEE Comput. Cardiol., 1984: p. 167-170.

31. Hodgkin, A.L. and A.F. Huxley, A quantitative description of membrane current and its application to conduction and excitation in nerve. J Physiol, 1952. 117(4): p. 500-44.

32. Rush, S. and H. Larsen, A practical algorithm for solving dynamic membrane equations. IEEE Trans Biomed Eng, 1978. 25(4): p. 389-92.

33. Fox, J.J., J.L. McHarg, and R.F. Gilmour, Jr., Ionic mechanism of electrical alternans. Am J Physiol Heart Circ Physiol, 2002. 282(2): p. H516-30.

34. Qu, Z., et al., Scroll wave dynamics in a three-dimensional cardiac tissue model: roles of restitution, thickness, and fiber rotation. Biophys J, 2000. 78(6): p. 2761-75.

35. Fenton, F. and A. Karma, Vortex dynamics in three-dimensional continuous myocardium with fiber rotation: Filament instability and fibrillation. Chaos, 1998. 8(1): p. 20-47.

36. Berenfeld, O. and A.M. Pertsov, Dynamics of intramural scroll waves in three-dimensional continuous myocardium with rotational anisotropy. J Theor Biol, 1999. 199(4): p. 383-94.

37. Wu, R. and A. Patwardhan, Restitution of action potential duration during sequential changes in diastolic intervals shows multimodal behavior. Circ Res, 2004. 94(5): p. 634-41.

38. Franz, M.R., et al., Cycle length dependence of human action potential duration in vivo. Effects of single extrastimuli, sudden sustained rate acceleration and deceleration, and different steady-state frequencies. J Clin Invest, 1988. 82(3): p. 972-9.

39. Tolkacheva, E.G., J.M. Anumonwo, and J. Jalife, Action potential duration restitution portraits of mammalian ventricular myocytes: role of calcium current. Biophys J, 2006. 91(7): p. 2735-45.

40. Rohr, S., J.P. Kucera, and A.G. Kleber, Slow conduction in cardiac tissue, I: effects of a reduction of excitability versus a reduction of electrical coupling on microconduction. Circ Res, 1998. 83(8): p. 781-94.

41. Rohr, S., Role of gap junctions in the propagation of the cardiac action potential. Cardiovasc Res, 2004. 62(2): p. 309-22.

42. Cannell, M.B., H. Cheng, and W.J. Lederer, Spatial non-uniformities in [Ca2+]i during excitation-contraction coupling in cardiac myocytes. Biophys J, 1994. 67(5): p. 1942-56.

43. Cleemann, L., W. Wang, and M. Morad, Two-dimensional confocal images of organization, density, and gating of focal Ca2+ release sites in rat cardiac myocytes. Proc Natl Acad Sci U S A, 1998. 95(18): p. 10984-9.

44. Lopez-Lopez, J.R., et al., Local calcium transients triggered by single L-type calcium channel currents in cardiac cells. Science, 1995. 268(5213): p. 1042-5.

45.   Niggli, E., Localized intracellular calcium signaling in muscle: calcium sparks and calcium quarks. Annu Rev Physiol, 1999. 61: p. 311-35.

46.   Wier, W.G. and C.W. Balke, Ca(2+) release mechanisms, Ca(2+) sparks, and local control of excitation-contraction coupling in normal heart muscle. Circ Res, 1999. 85(9): p. 770-6.

47.   Coombes, S., R. Hinch, and Y. Timofeeva, Receptors, sparks and waves in a fire-diffuse-fire framework for calcium release. Prog Biophys Mol Biol, 2004. 85(2-3): p. 197-216.

48.   Stern, M.D. and H. Cheng, Putting out the fire: what terminates calcium-induced calcium release in cardiac muscle? Cell Calcium, 2004. 35(6): p. 591-601.

49.   Saffitz, J.E., et al., Tissue-specific determinants of anisotropic conduction velocity in canine atrial and ventricular myocardium. Circ Res, 1994. 74(6): p. 1065-70.

VITA

SANJIV RAMALINGAM

Date of Birth: February 22, 1981
in
Mettur, India

Degree Awarded
Bachelors of Science in Electronics and Communication Engineering

Madurai Kamaraj University, April 2002